FEASIBILITY STUDY FOR A MANNED ELECTRIC MULTICOPTER CROSSING THE ENGLISH CHANNEL

Manuel Keßler, Bjoern Annighoefer, Walter Fichter, Michael Frangenberg, Wolfgang Granig, Hello Haas, Bastian Luettig, Ronald Stärz, Andreas Strohmayer

Abstract

Air taxis have been in a highly dynamic development phase for the last few years. Many configurations exhibit a multicopter layout, between 4 and 18 propellers for lift generation. Although favorable for its VTOL capability, the concept is not optimal for long range and endurance, with unknown limits. For our project study, we considered a specific mission: Moving a single human across the English Channel. Our question is, whether this goal would be achievable with a battery electric drive train, and what design constraints and operational boundary conditions need to be considered.

For range extension, cruise lift from additional wings proved beneficial, and the result for optimal target speed was quite high, even for this multicopter configuration. In addition to aeromechanics, flight mechanics and stability issues of the aircraft, structural design matters, pilot interface, and power management were considered. Hardware components were built, tested and integrated into an „Iron Bird“ demonstrator. Furthermore, for pilot interface development a moving simulator platform was built. Unfortunately, permit to manned flight proved to be the most challenging task, with no definitive solution yet.

1. MISSION AND BOUNDARY CONDITIONS

In order to assess the capabilities of multicopters for actual payload transport, a specific mission was defined: Manned flight over the English Channel. Preliminary analysis indicated quickly, that this distance of about 34km is just at the edge of battery powered technology, and such set the stage for several players at University of Stuttgart, Infineon, MCI Innsbruck and HybAir to accomplish this highly ambitious goal. A view of a possible flight-path is shown in Fig.1.

Fig.1: Shortest flight route from Great Britain to France to cross the English Channel

The participants brought in their specific expertise and knowledge to optimize, design, develop and construct such an aircraft. Although a hybrid electric power train using fossil fuels would have simplified the challenge, battery power was specified from the start. The same holds for the multicopter configuration, resembling more or less a „flying motorbike“.

Further considerations about certification or legal operation and available budget led to the decision to stay within the limits of the ultralight category according CS-VLA, restricting the maximum take-off weight to 600kg [1].

2. DESIGN AND DEVELOPMENT

Available energy and its optimum use is clearly a limiting factor for battery powered aircraft. For fixed wing aircraft it is obvious that range increases with additional battery capacity and weight. For VTOL the superlinear increase of power with additional weight restricts the ratio of battery to total mass to two thirds, in theory, beyond which endurance decreases again.

Nevertheless, in practice less than half the MTOW can be spent for batteries. In addition, large batteries are available and best handled as discrete packages. With some very rough estimates regarding component weights, it was decided to use 4 packs of 68kg each, providing a total energy of 44kWh, 37kWh of which can be drained.

2.1. Configuration

The multicopter configuration was defined as a requirement, as much as the battery electric power train. In addition, the impression of a “flying motorbike” should be visible as much as possible. Remaining degrees of freedom regarding the layout were the number of rotors, their actual placement and the possible addition of lift and control surfaces.

Utilizing general scaling analysis and simple generic parameter dependencies, several variants were investigated, namely a quad-, hexa- and octocopter, all in single and coaxial configuration. Although the octocopter provided the largest disc area and such had the most efficient thrust generation in hover, the additional structure and corresponding weight led to the decision for a quadcopter. However, for redundancy considerations a

doi: 10.25967/570141

coaxial configuration was chosen, in order to allow at least a controlled descent in case of single failure instead of total loss of control.

2.2. Aeromechanics

At the start of the project the feasibility of the mission was very questionable. First estimates under preliminary assumptions indicated an energy demand exceeding 50kWh, clearly beyond the amount available, and not considering any safety margins yet.

Consequently, significant power optimizations were required. Disc loading is the primary efficiency parameter in hover, so propeller diameter was increased. However, in forward flight at high speeds the gains diminish, as some simple blade element calculations indicated.

Such blade element analyses allowed the creation of generic performance maps for the propellers, including the primary dependencies on diameter, RPM, flight speed, and pitch angle on the loads of interest, namely thrust and drag, as well as power required. These performance relations were included into a spreadsheet to identify an optimal aeromechanic design as well as operational parameters for the primary mission task element cruise flight and a small hover phase at start and landing.

These two flight conditions of hover and high speed are of primary interest for the specified mission. This raised the question of the optimal flight speed for maximum range. In general, for every rotorcraft the power curve over speed has a “bathtub” shape, starting from high power demand in hover. With increasing velocity, power required decreases due to inflow effects on the rotor(s), reaching some minimum number at moderate speeds, and then grows rapidly, approaching a v^3 law ultimately. In addition, to overcome the increasing drag of the airframe, the pitch angle of the rotor(s) grows with speed squared, approximately. The exact numbers vary with the specific parameters and configuration, of course, but the qualitative behaviour is all the same. Fig. 2 shows the curves for the finally chosen design.

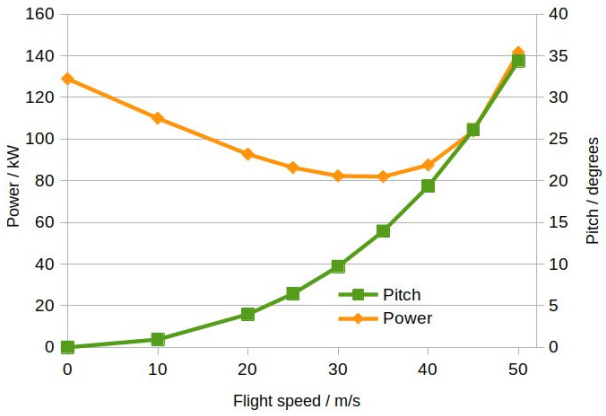

Fig. 2: Pitch and power curve of final design

From this figure obviously, the power required for hover can be taken as about 130kW (mechanical drive power), and the optimal velocity for maximum range occurs at the tangent from the origin to the power curve, in this case at 40-45m/s. For cruise, some 95kW are needed, and pitch angle is around 22°, which is quite considerable. The high speed may be surprising at first, but is a consequence of the high power requirements at low speeds, which necessitates the mission to be as short as possible.

Fig. 3 shows the dependency of required energy versus cruising-speed as well as the resulting flight-time for a distance of 34km without consideration of additional energy used for rise to any defined safety-height and final descend to ground This graph shows the lowest energy required for a speed of appr. 40 m/s and a flight time of appr. 14min.

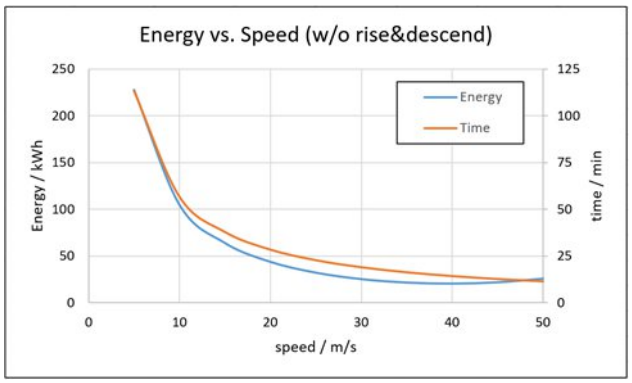

Fig. 3: Required energy and flight time versus cruising speed for a distance of 34km without consideration of rise and descend.

With the help of the spreadsheet various deliberations were taken. The dependence on propeller number and diameter, airframe drag area, and mass on energy consumption was investigated for a mission with reasonable safety margins for range and hover time. By trimming RPM and pitch angle, balance of vertical and horizontal forces was achieved to find reasonable operation conditions.

While getting closer to the energy budget, it still remained marginal, at best. So additional wings were considered for lift compounding, where the high speed helps to keep the surface area and thus additional weight low. Designing the wings as lifting surface around the beams carrying the motors and propellers integrates them at little additional weight. Exploration of different wing areas including their drag led to the final layout of Fig. 4 as a tandem configuration for the wings, to fully take advantage of the beam structure. Slightly more than one quarter of the lift required is generated by the wings under nominal cruise conditions.

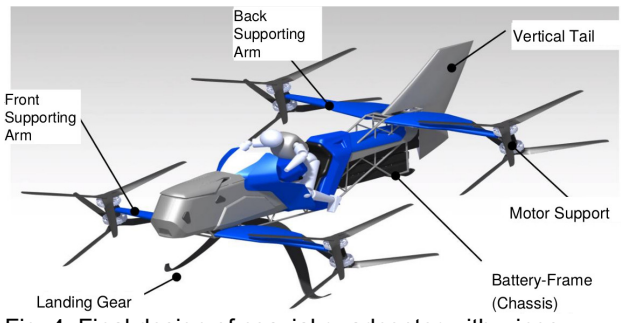

Fig. 4: Final design of coaxial quadcopter with wings

Key aspects here are that with increasing wing area and thus lift not only the drag rises, but at the same time propeller thrust necessarily decreases. However, the forward force required to counter the total drag (slightly) increases, leading to larger pitch angles for the rotors. In contrast, for hover and consequently at start and landing, the rotor angle is close to zero, which results in a large variation of rotor pitch angle from hover to cruise. To reduce complexity and weight, no motion of the propeller axis with respect to the airframe is possible, so on ground and in hover the nose points significantly upward, approaching the horizon in cruise.

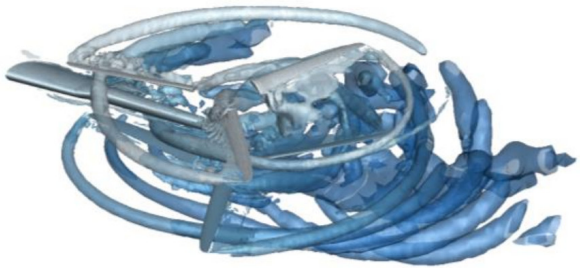

Fig. 5: Vortex visualization at cruise ($\lambda_2$criterion)

Further high fidelity CFD analyses as shown in Fig. 5 helped to optimize the angle of attack for the wings at several span stations and the orientation of the propeller axis, taking into account their respective interference. They also provided valuable data about load averages and their dynamic variation for the structural design and dimensioning of the beams.

In summary, the aeromechanic optimizations including the configuration change to lift compounding reduced the total energy estimate for a 40km mission with 120s hover time down to about 30kWh. Even considering some reasonable losses from battery to drive shaft, this is well within the battery budget of 44kWh.

2.3. Control

A multicopter has unstable flight characteristics and needs active control. For this purpose, the following digital flight control system has been designed. Since a loss of flight control is likely to have catastrophic consequences, an existing multi-purpose avionics flight control computer has been selected as the base-line.

The flight control system implements the control function. It consists of a central flight controller, the 8 engine controllers, inertial measurement unit and analogue sticks that read the pilot's commands.

The central flight control computer commands and receives information from each of the engine controllers individually. The computer hosts an airworthy hard real-time operating system and two partitions, the system partition and the telemetry partition. Partitioning enables a safety-critical segregation of essential flight controls and supportive telemetry.

The computer uses a configuration file, a so-called interface control document, to configure its partitions, interfaces and bus messages.

2.3.1 System Partition

The system partition performs multiple tasks: a) aggregates and transforms all sensor, engine controller and pilot input, b) executes the control law, c) commands the engine controllers, and d) sends data to the telemetry acquisition system.

The overall execution time is limited to 500µs per cycle, which was achieved when function d) is moved into its own partition. The computer executes the partition every 16ms.

2.3.2 Control Algorithm

The control algorithm has been designed in Matlab Simulink. Its main function is to control the pitch and roll attitude, the yaw rate and the vertical speed of the vehicle. The vehicle was designed to have a simple control interface, so the pilot only has to command the following values:

- Vertical speed
- Pitch angle (proportional to forward speed)
- Change in direction

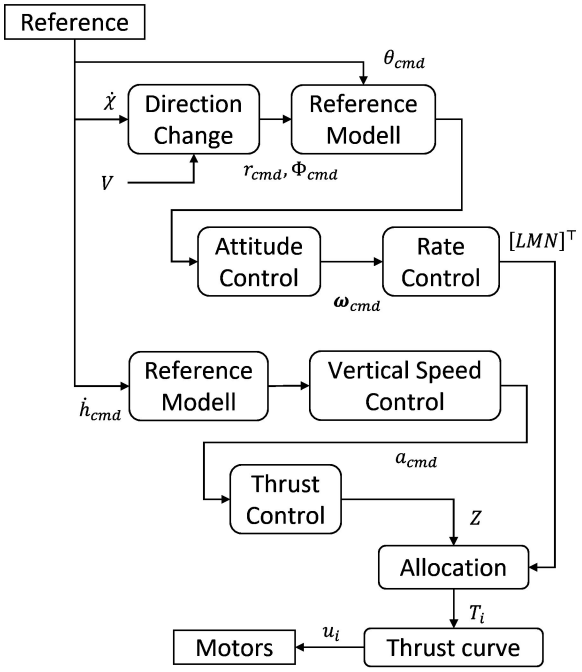

Fig. 6: Controller structure

Fig. 6 shows the internal design of the controller. The desired change in direction is first converted into a roll angle and yaw rate depending on the current speed. All the reference values are run through a second order reference model which ensures the vehicle can follow the commands in a reasonable manor without for example large overshoots. In addition, this decouples the perceived flight characteristics for the pilot from the controller settings that dictate disturbance rejection.

The output of the controller consists of three torques around all three axes and a total thrust. These are then distributed to the 8 motors using a pseudo-inverse, yielding individual thrust commands for each motor. Using the thrust curve shown in Fig. 15 this thrust is converted to a motor command.

An engine failure is a critical event for any multicopter as it can cause the vehicle to lose control within less than a second. In the event of such a failure being detected by the ESCs, the allocation can be changed during flight. To avoid large asymmetries in the allocation, the diagonally opposed engine to the failed one is disabled as well. As the remaining thrust will probably not be sufficient to maintain altitude, this is mainly designed to avoid uncontrolled tumbling and aid the pilot in leaving the vehicle using a parachute. As shown in Fig. 7 the distribution therefore prioritizes the pitch and roll axes if the motors would be saturated.

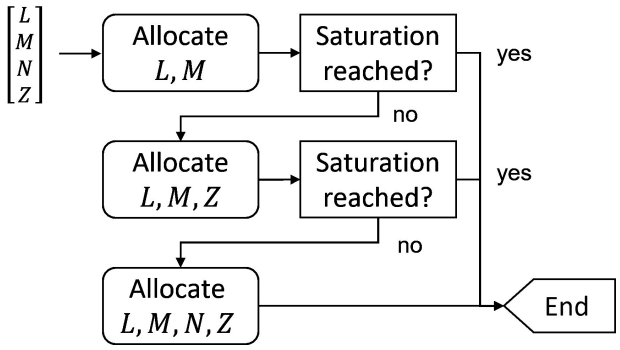

Fig. 7: Prioritization procedure during allocation

Because the control authority on the yaw axis is limited in a multicopter, relatively large differences in motor commands would be required for yaw control in cruise, which is inefficient. Therefore, yaw control is disabled at higher speeds and directional stability is provided by a fixed vertical stabilizer fin at the back of the vehicle.

To avoid potential errors during the implementation, code generation is used. This turns the Simulink model into C-code which is then inserted into a manually written wrapper in the partition. The wrapper is structurally very simple and mainly moves data into and out of the generated parts of the code.

2.3.3 Telemetry Partition

This partition aggregates telemetry data, i.e., engine commands and health information, sensor data, partition duration, and pilot's inputs. It then sends these via CAN to a telemetry device, which enables the recording and the active monitoring of the mission by the pilot and the ground crew. Following data are transferred via CAN interfaces and are sent to a base-station via telemetry:

8x Motor Temperatures
8x Rotor RPM
8x Inverter Temperatures
8x Inverter Input Currents
8x Inverter Input Voltages
8x Inverter Excitation Inputs
8x Inverter Status
1x Battery output Voltage
4x Battery Currents
4x Battery Temperatures
4x Battery State of Charge
4x Battery Status
3x IMU acceleration (x, y, z)
3x IMU angle (α, β, γ)
1x Pressure Height
3x GPS Coordinates (latitude, longitude, height)
4x Stick excitations (throttle, yaw, pitch, roll)
1x Boardcomputer Status

2.4. Structural design

The structural design of this high-speed manned multicopter is dominated by low drag requirements, which result in a very slim design, that is operated like a motorbike. The main weight and size of the core are taken by the batteries, two in the front part and other two in the rear part. The required high-speed operation results in a tilt-angle of the rotors relative to the main-frame, which is considered in the landing gear, see Fig. 8. Fig. 9 shows this slim setup from top including the wing-structure and rotor setups.

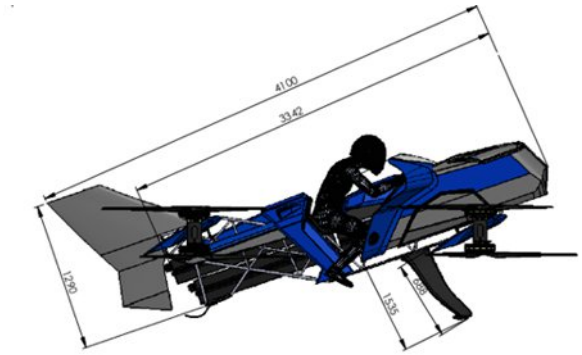

Fig. 8: Side view of the high-speed manned multicopter representing the main structure and tilted rotors as well as vertical stabilizer for high-speed operations.

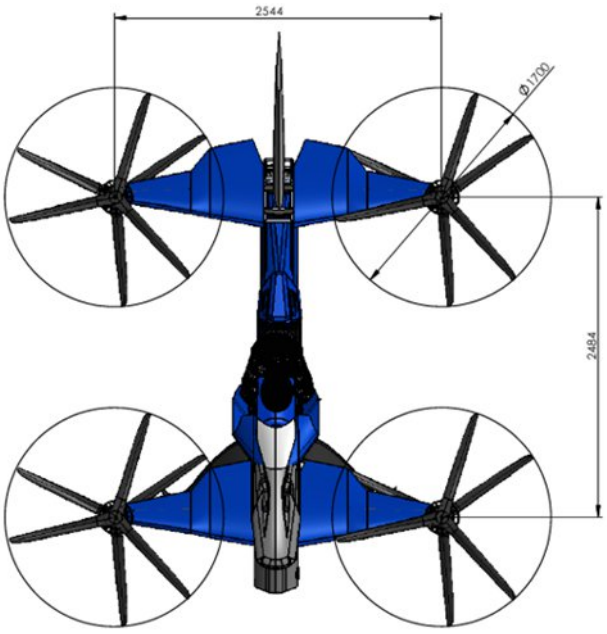

Fig. 9: Top view of the high-speed manned multicopter representing the wing- and rotor structures.

For further system analysis and optimization an estimation of the overall vehicle mass is required. Table 1 shows a collection of system components and their individual mass to summarize an estimated full system mass.

Table 1: Total vehicle mass estimation

		mass / kg	devices	total / kg
1	Propeller	1.85	8	14.8
2	Motor incl. Cabling	9.5	8	76
3	ESC	1.5	8	12
4	ESC Cables & Busbar	1	8	8
5	Cable Tree Battery	2	4	8
6	HV-Battery	68	4	272
7	Mainframe	38	1	38
8	Arms&Wings	6.5	2	13
9	Vertical Stabilizer	3	1	3
10	Cover&Windshield	5	1	5
11	Landing Gear	5	1	5
12	Cockpit	4.3	1	4.3
13	Boardcomputer&Sensors	3.8	1	3.8
14	Aux Supply (Bat&DCDC)	2.4	1	2.4
15	Safety (Relais)	4	1	4
16	Pilot	78	1	78
17	Safety Equipment	13	1	13
	Total Takeoff Mass			**560.3**

The largest forces of this vehicle must be taken by the front wing structure, see Fig. 10. To ensure a proper optimization of low weight and sufficient robustness for all flight conditions verification was performed via FEM-Simulations, see Fig. 11. and real force-tests on ground. All airworthiness requirements of mechanical tensions on wings were fulfilled.

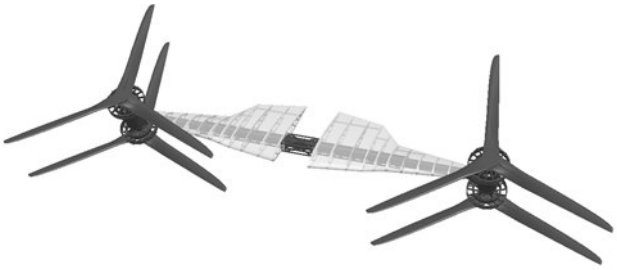

Fig. 10: Front wing structure and design.

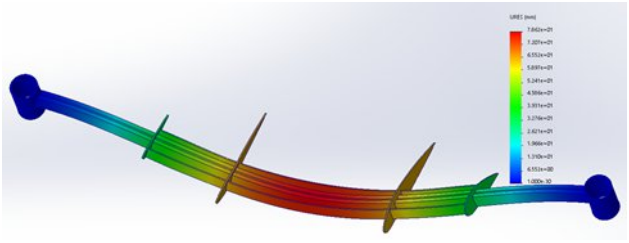

Fig. 11 FEM-Simulations of simulated load on the front wing structure.

2.5. Electrical System Overview

The electrical system design mainly contains the entire powertrain, the boardcomputer with flight-controller software, and the pilot-interface like control sticks and flight display. Additionally, this system is equipped with a startup and backup-battery for auxiliary supply, aeronautical radio communication system and a telemetry system transferring system parameters to a central ground-station for supervision and monitoring the state of health. A drawing of the whole system can be found in Fig. 12.

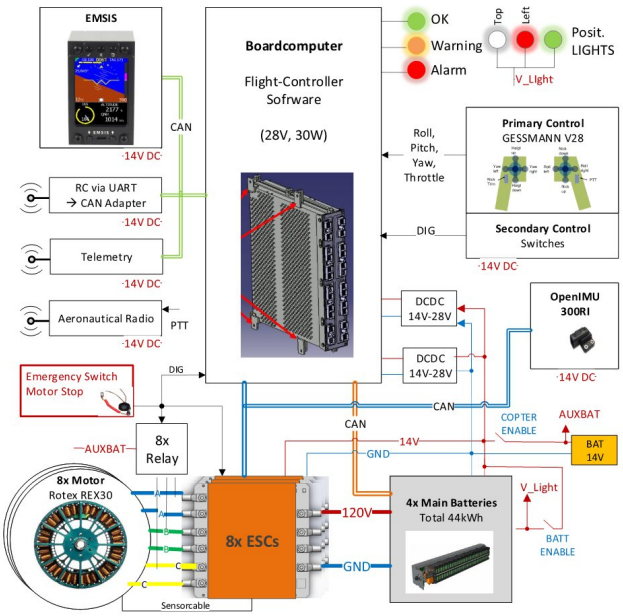

Fig. 12: Overall system block diagram of the manned multicopter electronics.

2.6. Pilot interface

The pilot interface to this aircraft beside main switches to turn on the copter can be separated in two parts. First the pilot can operate the multicopter via safety-certified thumb-sticks including additional buttons for trimming and radio communication push to trigger (PTT) functionality [2]. The second interface are visualizations of relevant technical and navigational parameters. This is realized by the avionic EMSIS device, where the visual data-view was adapted to this mission need. An overview of the planned cockpit can be seen in Fig. 13.

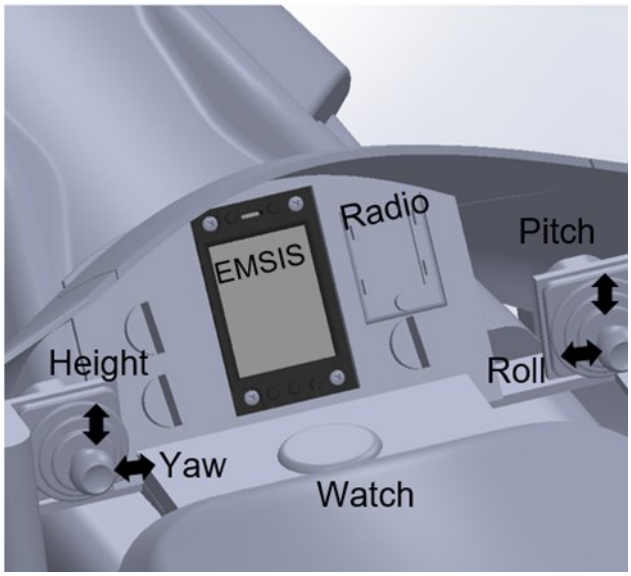

Fig. 13: Cockpit view of the manned multicopter

2.7. Drive train and power management

The drivetrain and overall power management is one of the most critical parts of this project. A block diagram of the drivetrain can be seen in Fig. 14 where a schematic of the electrical power-path from batteries via electrical speed controllers (ESCs) to the motors and propellers can be seen. In this figure also parasitic resistances are drawn which are limiting the performance additionally.

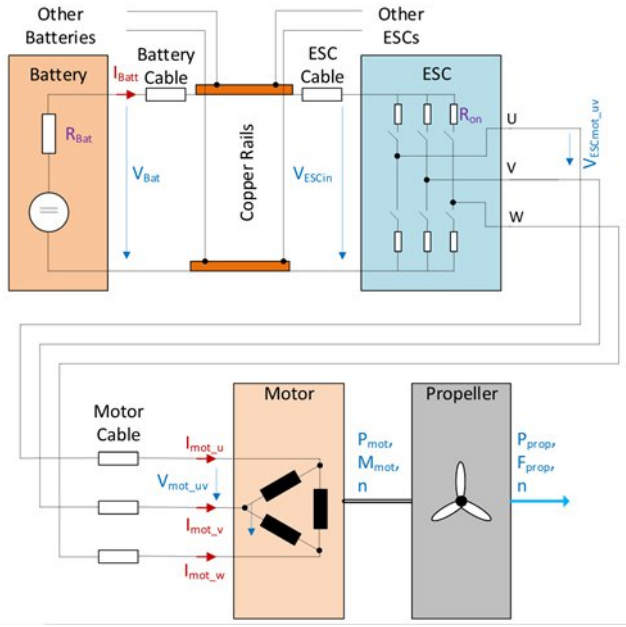

Fig. 14: Block diagram of the drivetrain from batteries via ESCs, Motors and Propellers including parasitic resistances.

The overall system performance from power input to generated thrust for the whole multicopter can be seen in Fig. 15. Here we can see that for just hovering approximately 560 kg about 95% throttle input is required, drawing a power of 136kW. In this configuration there is no headroom for acceleration or voltage drop of the batteries during the flight. Additional power required in case of turbulences was considered, but omitted at first [3].

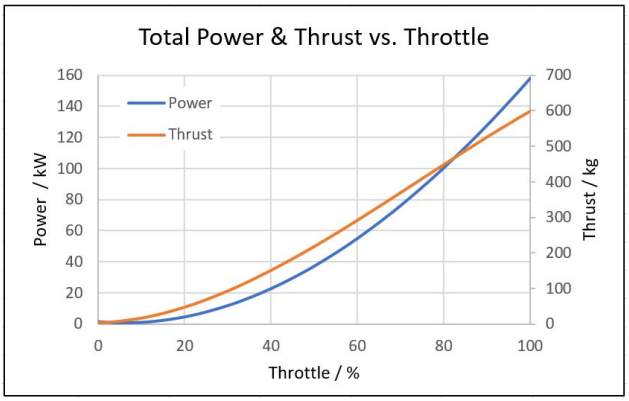

Fig. 15: Total Power and thrust generated by the planned powertrain dependent on throttle excitation.

The performance of the powertrain was also significantly limited by loss-resistances because the used permanent magnet synchronous machines have a rotational speed linearly dependent on voltage. Together with the nonlinear characteristic of lift-force related to rotational speed, a voltage drop below a certain limit renders hovering flight impossible due to low thrust generated by the powertrain. Beside the limited energy stored in the batteries also this effect limits the overall flight time and usable energy for real flight. Fig. 16 shows the characteristic of required current related to battery voltage to maintain hovering. The usable range of battery-voltage is limited down to 105V only, which can cause problems for landing after a certain flight-time with decreasing battery-voltage.

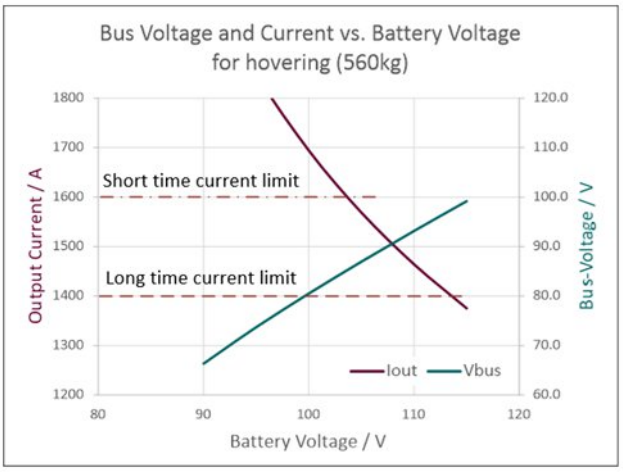

Fig. 16: Required current versus battery-voltage to maintain hovering including indication of operational limits.

2.6.1 Flight profile

As the mission is just at the edge of technically feasible, certain real world adjustments are in order to actually reach the goal, in this case literally the opposite coast. Here, the possible power output of battery technology decreases while discharging, sparing only a minimum at the end, while power required for the final hover before hitting the ground is maximal again.

Initial cruise height considerations delivered only marginal gains at achievable heights for their lower air density, as the climb and descent phases mostly cancel each other in terms of energy consumption. However, instantaneous power required is different. In the climb phase, the potential energy gain adds some more power drain, which is then reduced in the later descent and approach phase. At cruise speed, every degree of climb requires about 5kW additional power, and each descent equivalently less.

In consequence, momentary power can be adjusted within limits to the discharge curve of the batteries. From manufacturer's data, for a total discharge duration of approximately 20 minutes (3C), after reaching safe height out of hover and accelerating to cruise speed, a starting climb angle of 3° seems reasonable, with a linear decrease over the flight duration, up to 3° descent before landing. The corresponding height profile is mostly parabolic with a

maximum height of about 700m. Even in the case of insufficient power for a final hover before ground contact, generic emergency procedures pitching the aircraft (nose up) and thus reducing speed by converting kinetic energy into propeller thrust, somewhat similar to a helicopter auto-rotation, could ensure a safe landing with non-fatal impact velocity.

3. HARDWARE AND TESTING

To test the whole system before assembly and operation of the final manned multicopter several test structures as well as test operations were performed.

3.1. Components

Main system components used:

Propellers:	8x H30F1.5, Helix [4]
E-Motors:	8x REX30, Rotex [5]
Inverters:	8x TMM280120-3EI, MGM-Compro [6]
Batteries:	4x VL-28s37p, Voltlabor [7]
Bordcomputer:	RDC, Diehl Aviation [8]
IMU:	OpenIMU300RI, ACEINNA [9]
Flight Display:	EMSIS 3.5inch, Kanardia [10]
Control Sticks:	V28-P-Z-B10-E2142, Gessmann [11]
Remote-Control:	Tanaris Q X7, FRsky [12]
Telemetry:	WLAN based, Riedel Electronics [13]
AUX Battery:	LiFePo4 8400mAh 4S2P, ZIPPY

3.2. Propeller tests

Initial questions on the optimum propulsion with propellers operated in non-axial air-flow configuration were analyzed by propulsion-tests on a moving test platform [14][15]. This test-platform has been an automotive pick-up applied with propulsion frame and force measurement setup to measure the influence of air-speed to the operation and performance for different propeller-types. A picture of this setup can be seen in Fig. 17.

Fig. 17: Measurement setup for propeller performance tests on a pick-up truck as moving test platform.

The outcome of these tests was that 2-blade propellers generated too much of mechanical vibrations for safe and economic operation. Therefore 3-bladed propellers were used for further tests because of their much lower tendency for vibrations. Fig. 18 show the result of lift-force versus air-speed for an air-flow angle of 0° (Air-flow perpendicular to the propeller axis).

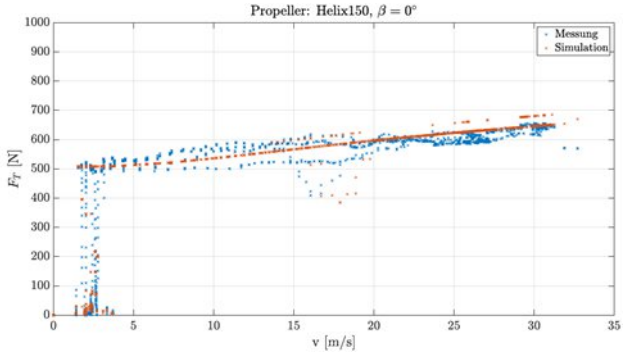

Fig. 18: Lift-force of a 3 bladed propeller with a diameter of 1.5m and an air-flow angle of 0°.

3.3. Iron Bird demonstrator

For first propulsion, control and flight tests a simple demonstrator was built. This demonstrator was manufactured with simple and easy to use steel sections intentionally not focusing on weight optimization but with focus on functionality and observability – therefore the name “IRON BIRD”. A picture of the Iron Bird is shown in Fig. 19, where one can see the 4 arms equipped with 2 motors and propellers each, mounted on a central frame containing the motor inverters (electrical speed controllers – ESCs) and flight controllers.

Fig.19: IRON BIRD demonstrator with target propellers, motors, inverters, boardcomputer and flight-controller software.

Several ground- and hovering flight tests were performed with this demonstrator to get more insight about the overall system performance as well as controllability. For this reason, a telemetry system was applied to this platform to transfer all relevant CAN messages to a ground-station for online monitoring during flight as well as for logging and post-processing of relevant data. Fig.20 shows a picture of a hover-flight to test the propulsion performance as well as the controllability.

Fig. 20: IRON BIRD in hover-flight for performance test and data-logging of relevant data for post-processing.

3.4. Moving simulator platform

For behavioral tests of the flight-controller software as well we to train the pilot for operating this manned multicopter, a 6 degree of freedom (6DOF) simulator platform was built [16]. Additionally, the placement, position and operation of seating as well as the control-interface via control-sticks could be tested and their arrangement optimized with this simulator platform. Fig 21 shows a picture of operation with a pilot, where the pilot was equipped with 3D-goggles for environmental view and the operators outside could follow the view of the pilot via external monitors.

Fig. 21: 6DOF simulator platform to test the flight-controller software, vehicle control and seating.

A functional software and signal flow-chart can be seen in Fig. 22. The pilot inputs were used as steering-inputs to the flight controller firmware implemented in Matlab [17]. Matlab generates signals for the visualisation in XPLANE [18] as well as control-signals for the 6DOF platform. XPLANE is then projecting the visual flight scenery onto 3D goggles. To ensure a correct flight feeling, one hand controller of the 3D visualisation was put on the copter to operate as motion-compensation reference for the 3D goggles used by the pilot.

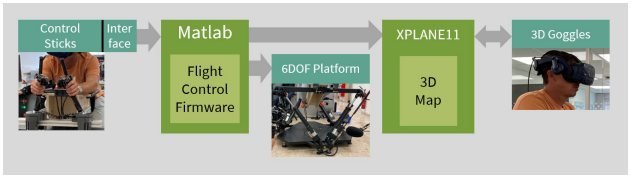

Fig. 22: Functional software and signal flow-chart of the simulator platform.

4. CERTIFICATION EFFORTS

A legal manned flight requires at least a Permit-to-Fly, which was our “certification” goal. This requires to conduct at least some qualification activities from what is necessary for regular type certification. What is exactly necessary was discussed with the certification authority.

The certification basis is divided into structural aspects and the flight control system aspects.

We opted to classify the copter as CS-VLA and to apply certain aspects from SC-VTOL due to the more complex nature of the flight control system. In an initial assessment, we investigated the potential main failure contributors and found a preliminary systems architecture, shown in Fig. 23.

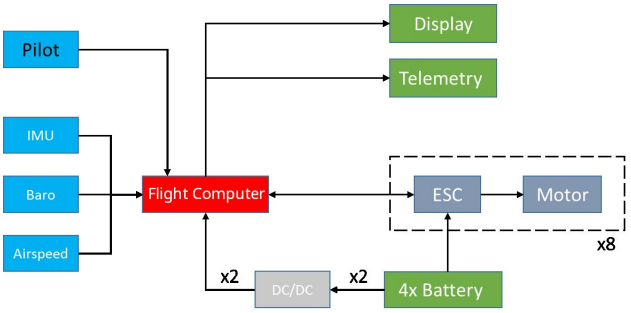

Fig. 23: Preliminary system architecture for assessment

With this architecture and the mission profile, we conducted a functional hazard assessment based on ED-279 draft [19]. We quickly found that many functional failures would either result in catastrophic events or require an emergency system, e.g., a parachute, or a ballistic recovery system. Furthermore, software errors have a direct potential for catastrophic failures.

We integrated an emergency stop function into the concept. The pilot can trigger this via pulling a safety plug that is attached to the pilot, similarly to the system used on jet skis. The system then stops all motors by a) killing power and b) shorting out the motor windings using normal closed (NC) contactors, which decelerates the rotors instantly. The pilot will then evacuate using a parachute. A verification test for this emergency stop function was scheduled to demonstrate sufficiently fast motor stop that would ensure the pilot could evacuate uninjured and limit damage to the surrounding environment.

To address potential hardware requirements, we incorporated a close-to-certified central computer featuring an ARINC 653P4 operating system and thus both time and spatial partitioning.

We then conducted an FMEA to produce more detailed reliability and integrity figures. We found a probability of 6e-4 for any failure that would trigger the emergency stop during the mission. A portion of these would then – depending on the mission phase - lead to catastrophic failures, as the pilot cannot disembark and use a parachute, for the altitude is insufficient for a ballistic recovery system.

As per our estimate, the main contributors are the central computer, motors and engine control units and the battery packs. However, acquiring actual reliability numbers posed a challenge. Most manufacturers do not have these numbers around, especially not in instationary operating modes. Furthermore, we did not find any actual source for battery pack reliability and assumed 1e-4 per hour.

We then condensed the FMEA into an FMES (Table 2). Failure Effects are additionally classified if the emergency stop function should be triggered.

Table 2: Failure Mode Effects Summary

Failure Effect Vehicle	Emergency Stop?	Probability
Loss of Control	yes	1,4582E-5
Degraded safety margin	no	2,5300E-6
Motors stop	yes	9,7000E-5
Vehicle descends	yes	3,4400E-4
Vehicle detects, emergency program	yes	1,0811E-4
Vehicle must not start	no	7,0400E-5

Still, the emergency stop function does not work for the early and late stages of the flight – whenever the vehicle is too low to safely deploy the parachute. The exposition duration is tightly coupled to the flight profile. Next, we drafted a Plan for Software Aspects of Certification (PSAC).

4.1. Requirements

After discussion with the authority, the hazard assessment and preliminary FMEA, classification as CS-23 Class I and application of AC-23.1309-1E [20] was demanded. This requires development to at least DAL C and 1e-6 for the flight control system and the absence of single point failures that could lead to catastrophic events. The parachute emergency procedure cannot be accepted as mitigation procedure, because not mitigating in all situations.

These requirements could not be met for this weight restricted, budget-limited, single service and experimental multicopter, as already the cost for DAL D software development would have amounted to an estimated man-year in development and certification effort.

4.2 Testing Plan

In order to achieve reasonable confidence in software correctness, we planned to use three different levels of testing:

1. simulation in simulink (MiL)
2. execution of generated software on computer, peripherals simulated (SiL)
3. execution on flight computer in a HiL setting, peripherals are simulated via CAN
4. execution on the iron bird, unmanned vehicle

For each setting, we aimed to execute the same scenarios: a) descend and climb at different angles at optimal speed; b) acceleration from hover to optimal speed to hover.

This should ensure to find coding errors as early and with as little risk as possible.

4.3 Way Forward

Given an actual commercial manned multicopter project in Europe, with certification in mind and sufficient funds to perform DAL C system development, the requirement towards single point failures poses the greatest challenge. In the current design, there are several components that have the potential for catastrophic behaviour: a) flight control computer, b) battery packs, c) engine controllers, d) IMU sensors. Academically speaking, the flight control computer requirements demand at least a dual-duplex or quadruplex configuration. Due to the unstable nature of multicopters, the pilot cannot switch-over the computers manually and thus the system must perform this automatically – and quickly. With respect to batteries, the multicopter must bring more battery packs than needed, which increases overall weight and in turn power requirements. For engine controllers, only select models are available for the use case. Most controllers work best in stationary operation, i.e., at their rated power. The multicopter use case demands flexible power flow – and to give room for actual steering, the power flow during normal flight is about 60-70% of the rated power.

5. CONCLUSIONS AND OUTLOOK

A multicopter being capable of carrying one person across the English Channel has been designed, developed and partly built. Strict energy and power constraints necessitated optimizations of the configuration as a whole as well as on individual component level. Practicability and safety considerations were driving other design decisions. For flight mechanical validation an Iron Bird demonstrator was built and flight tested, with high speed testing yet missing. In hover, agreement with analysis and simulation was good, but the drive train reached its limits at several points, demanding some elaborate adaptations.

In parallel, construction of the final assembly took place, including structural testing of the wings. Furthermore, for pilot training and handling qualities assessment a moving simulator platform was built, including visual immersion and motion feedback in addition to exploring placement of controls and general usability.

Besides the final constructing and tests necessary to prove the technical capability of the aircraft, which will take place remotely piloted on flight test areas, currently the ultimate blocker is to obtain a permit for manned flight. The requirement to prove failure rates and development procedures quite similar to commercial aircraft for such a one-of-a-kind flight with a voluntary pilot over blocked ground turned out to be a show-stopper for the project, unfortunately, due to limited resources. Final tests are planned to get at least reliable performance results of Iron Bird flights at higher speeds, because only hovering tests were done up to now. Further work on the aircraft thus depends on creative application ideas, as the initial mission is out of reach.

References

[1] CS-VLA Very Light Aeroplanes, „Easy Access Rules fir Very Light Aeroplanes (CS-VLA)“, EASA, 2003

[2] Yanik Romer, „Modellierung und Analyse von Bedienelementen für bemannte Multikopter“, Master Thesis Universität Stuttgart – Institut für Flugmechanik und Flugregelung, 2021

[3] Sebastian Gieray, „ Analyse des Energieverbrauchs von Schwerlast Multikoptern bei Turbulenzen“, Master Thesis Universität Stuttgart – Institut für Flugmechanik und Flugregelung, 2021

[4] Helix, Propellers, www.helix-propeller.de

[5] Rotex, Permanent Magnet Synchronous Motors, www.rotexelectric.eu

[6] MGM-Compro, Inverters, www.mgm-compro.com

[7] Voltlabor, Batteries, www.voltlabor.com (www.mibabattery.com)

[8] Diehl, Boardcomputer (Remote Data Concentrator), www.diehl.com/aviation/en/portfolio/avionics

[9] OpenIMU, IMU, https://www.aceinna.com/inertial-systems/TILT

[10] Kanardia, EMSIS, https://www.kanardia.eu/product/emsis/

[11] Gessmann, Control Sticks, https://www.gessmann.com/application/industrial-joysticks/

[12] FRsky, Remote Control, https://www.frsky-rc.com/product/taranis-x9d-plus-2/

[13] Riedel Electric, Telemetry, https://www.riedel.net/

[14] Moritz Berres, “Entwicklung einer skalierbaren Simulationsumgebung für den Antriebsstrang von Schwerlast-Multikoptern“, Master Thesis Universität Stuttgart – Institut für Flugmechanik und Flugregelung, 2020

[15] Mohamed Amine Ben Salem, „Aerodynamische Modellierung von Multikopter Propellern und Verifizierung anhand von Flugtests“, Bachelor Thesis Universität Stuttgart – Institut für Flugmechanik und Flugregelung, 2021

[16] VRXsim, 6DOF Simulator Platform, www.vrxsim.com

[17] Matlab, Mathworks, www.mathworks.com

[18] XPLANE11, X-Plane, www.x-plane.com

[19] Draft ED-279 "Generic Functional Hazard Assessment (FHA) for UAS and RPAS", EASA, 2020

[20] 23.1309-1E - System Safety Analysis and Assessment for Part 23 Airplanes, FAA, 2011